



Contents lists available at ScienceDirect



Catalysis Today

journal homepage: www.elsevier.com/locate/cattod

Selective photocatalytic oxidation of aromatic alcohols in solar-irradiated aqueous suspensions of Pt, Au, Pd and Ag loaded TiO₂ catalysts

Sedat Yurdakal^a, Bilge Sina Tek^{a,*}, Çağlar Değirmenci^b, Giovanni Palmisano^c

^a Kimya Bölümü, Fen-Edebiyat Fakültesi, Afyon Kocatepe Üniversitesi, Ahmet Necdet Sezer Kampüsü, 03200, Afyonkarahisar, Turkey

^b Kimya Bölümü, Fen Fakültesi, Anadolu Üniversitesi, Yunus Emre Kampüsü, Eskişehir, Turkey

^c Department of Chemical and Environmental Engineering, Institute Center for Water and Environment (iWater), Masdar Institute of Science and Technology, P.O. BOX 54224, Abu Dhabi, United Arab Emirates

ARTICLE INFO

Article history:

Received 22 January 2016

Received in revised form 22 May 2016

Accepted 23 May 2016

Available online xxxx

Keywords:

Pt, Au, Pd and Ag loaded TiO₂

pH effect

Photocatalysis

Sun light

Green synthesis

Aldehydes synthesis

ABSTRACT

The photocatalytic partial oxidation of 4-methoxybenzyl alcohol (MBA) and 4-nitrobenzyl alcohol (NBA) to corresponding aldehydes or acids was performed in water under simulated solar light at different pH's by using Pt, Au, Pd and Ag loaded Degussa P25 TiO₂ catalysts, prepared by photoreduction. Bare Degussa P25 TiO₂ was also used as a reference. The metal loaded TiO₂ photocatalysts were characterized by XRD, TEM, ESEM and DRS techniques. The best activity and selectivity results were obtained with Pt loaded TiO₂. The reactivity results show that metal loading on Degussa P25 sharply promotes the photoactivity and product selectivity towards aldehydes. Moreover, at low pH's very high aldehyde selectivities were determined for both alcohols. MBA oxidation rate was very high at low pH's, whereas an opposite trend was observed for NBA, due to the difference of the substituent group. Only from NBA a significant amount 4-nitrobenzoic acid (ca. 50%) was obtained at high pH values.

© 2016 Published by Elsevier B.V.

1. Introduction

TiO₂ is the most used photocatalyst, since it is cheap, photoactive and resistant to photocorrosion [1,2]. Due to its wide band gap energy (3.0–3.2 eV), TiO₂ photocatalysts are active mainly under UV irradiation. TiO₂ may be used also under sun light because this radiation includes *ca.* 3–5% UV wavelengths [3]. By considering the energetic world strategy, and, given that sun light is a green and sustainable energy source, photocatalysts being active under sun light and in a green solvents as water can represent a good alternative to traditional thermal catalysis, usually performed at high temperature and pressure, and by using heavy metals as catalysts and harmful species as oxidants [2,4–7].

In order to increase TiO₂ photoactivity under sun light, loading by metals has been pursued [8–12]. This procedure affords absorbance in the visible region, so that both UV and visible radiation can activate the semiconductor catalyst [12]. In other words, metal loading can introduce intraband gap states, thus improving its ability to absorb low energy photons. In addition, the

photoactivity increase occurs *via* the delay of the recombination rate of photogenerated electron and hole pairs. However, a good absorbance in visible region gives of course no warranty for better photocatalytic activity under solar irradiation. Therefore, activity tests for the desired oxidation need to be performed with a case-by-case approach.

Although metal loaded TiO₂ photocatalysts have been widely used for degradation of harmful compounds under visible or solar irradiation [13–16], only a few investigations were carried out on their application in organic syntheses [17–19]. Shiraishi and co-workers investigated the photocatalytic synthesis of nitrosobenzene from aniline (90%) by using Pt loaded TiO₂ photocatalysts in toluene and under visible irradiation [19].

In that work, home prepared anatase and rutile TiO₂ photocatalysts were prepared loaded by Pt. Degussa P25 was also used for comparison. All Pt-loaded catalysts have significant absorbance in visible irradiation. Degussa P25 showed negligible photoactivity under visible irradiation due to the lack of absorbance of visible radiation. Zheng et al. [8] reported on the preparation of Au, Pt and Ag loaded home made TiO₂ by using a novel method and applied them to the selective photocatalytic oxidation of benzene to phenol in aqueous suspension and under visible irradiation. The metal loading procedure involved Ti⁴⁺ in TiO₂ being reduced to Ti³⁺ in

* Corresponding author.

E-mail address: sinabilge.t@gmail.com (B.S. Tek).

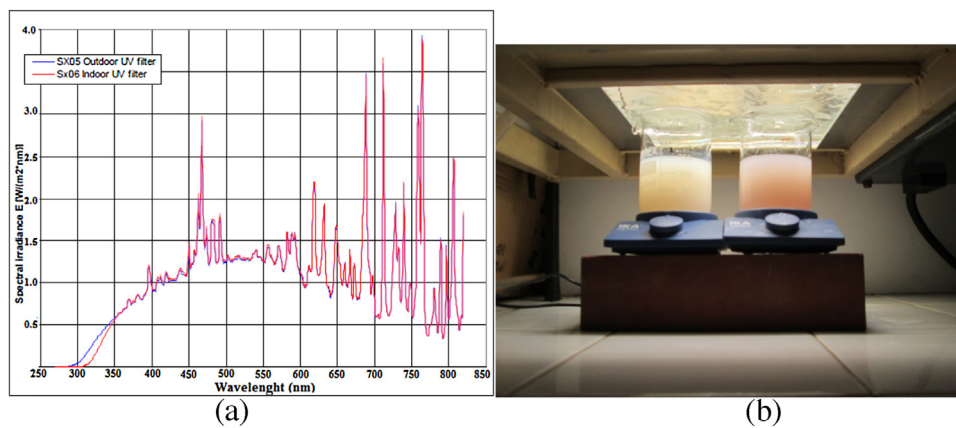


Fig. 1. The irradiation spectrum of solar simulator (1500W) (a) and used reactors (b) [4].

ethanol and, finally, the addition of a noble metal salt with the reduction of the noble metal cation carried out under dark by Ti^{3+} . High yield (63%) and selectivity (91%) for phenol production were obtained. A mechanism was suggested for oxidation of benzene on Au-loaded TiO_2 in which an electron transfers from Au nanoparticles to TiO_2 under visible irradiation, and Au^+ oxidizes phenoxy anions to form phenoxy radicals finally producing phenol.

Due to both low solubility of most of organic molecules in water and, also, to the generally low selectivity of the photocatalytic organic synthetic processes in water, photocatalytic synthetic reactions have been generally performed in organic solvents [20].

Selective oxidation of alcohol to carbonyl groups can be considered a key step in many organic syntheses [20]. The common practice to perform this oxidation usually consists in a catalytic process carried out in the presence of organic solvents at high temperature and pressure making use of stoichiometric oxygen donors that not only are expensive and toxic, but also produce large amounts of dangerous waste [2,4–7]. Moreover, huge amounts of heavy metals are generally used as catalysts. The elimination of these environmentally harmful conditions is, thus, one of the challenges of nowadays research. Recently, photocatalytic partial oxidation of aromatic alcohols to the corresponding aldehydes has been carried out under solar radiation in aqueous suspensions of home-prepared (HP) anatase and rutile TiO_2 . In those cases HP photocatalysts, containing high amounts of amorphous phase, showed selectivity values for aldehyde production far higher than those of commercial and crystalline samples [20–23].

In the present work, the photocatalytic oxidation of 4-methoxybenzyl alcohol (MBA) and 4-nitrobenzyl alcohol (NBA) was performed in water and under simulated solar light at different pH's. In order to increase TiO_2 activity and product selectivity, Me-loaded TiO_2 catalysts ($\text{Me} = \text{Pt}, \text{Au}, \text{Pd}$ and Ag) were home-prepared by photoreduction. Degussa P25 [24,25] and metal loaded Degussa P25 [19,26–28] were deeply investigated by many studies. The specific aim of the present work is to evaluate the influence of the different metals loaded on TiO_2 , of the suspension pH and of the substituent groups of benzyl alcohol on the performance of the photocatalytic process. The catalysts were characterised by XRD, TEM, ESEM and DRS techniques and their photoactivity was assessed by runs carried out in a batch reactor under sun light irradiation.

2. Experimental

2.1. Catalyst preparation and characterization

A suspension made of 2 L water, 500 mL ethanol, 10 g of Degussa P25 and the required amount of Pt, Ag, Au or Pd sources (PtCl_4

solution, AgNO_3 , AuCl or PdNO_3) was prepared. This suspension was then treated by ultrasounds for 15 min. Given the low solubility of AuCl , a stoichiometric amount of NaCl was added to the solution to promote the formation of the soluble complex $[\text{AuCl}_2]^-$.

For the photodeposition of the metals on TiO_2 an annular 2.5 L Pyrex batch photoreactor was used; it was filled with the above described suspension. The gas-seal photoreactor was provided with ports in its upper section for the inlet and outlet of gases. A magnetic bar guaranteed a satisfactory suspension of the photocatalyst and the uniformity of the reacting mixture. A 700 W medium pressure Hg lamp (Helios Italquartz) was axially immersed within the photoreactor and it was cooled by water circulating through a Pyrex thimble, so as to keep the temperature of the suspension at ca. 300 K. The aqueous suspension was continuously bubbled with Helium at atmospheric pressure; the gas was introduced in the reactor 30 min before turning the lamp on. The gas, the lamp and the agitation were maintained for 8 h. After waiting for the solid decantation, the liquid phase was separated from solid phase and the so obtained wet catalyst was washed two times by using 2.5 L batches of deionised water. Finally, the wet powder was dried at 100 °C and a fine powder was obtained. After drying, some batches were calcined in air at 400 °C for 3 h. Hereafter the catalysts are labelled as $\text{Me}-\text{TiO}_2-\text{X}\%-Y$, being Me the loaded metal, X its molar percentage and Y the treatment temperature (°C).

XRD patterns of the powders were recorded by a Philips diffractometer using the $\text{Cu K}\alpha$ radiation and a 2θ scan rate of $1.281^\circ \text{ min}^{-1}$. SEM images were obtained using an ESEM microscope (Philips, XL30) operating at 25 kV. A thin layer of gold was evaporated on the catalysts samples, previously sprayed on the stub from a suspension and dried at room temperature. UV-vis spectra were obtained by diffuse reflectance spectroscopy using a Shimadzu UV-2401 PC instrument. BaSO_4 was used as a reference and the spectra were recorded in the 300–600 nm range. TEM images were obtained using an HR-TEM instrument (JEM-2100). Before the analysis the samples were dispersed in deionised water by ultrasound treatment, deposited on a carbon-coated Cu grid, and dried at room temperature.

2.2. Photoreactivity setup and procedure

The photoreactor used for the runs carried out under simulated solar radiation was a 250 mL cylindrical beaker (diameter: 6.7 cm) containing 150 mL of aqueous suspension. A magnetic stirrer guaranteed a satisfactory suspension of the photocatalyst and the homogeneity of the reacting mixture. This photoreactor was placed inside a 1500 W solar light simulator equipped with a Xenon lamp and a reflector. The distance from the lamp to the suspension

top level was 27.5 cm. The values of the radiation energy impinging on the suspension, measured by using a radiometer (Delta Ohm, DO 9721), were 0.81 mW cm^{-2} in the 315–400 nm range and 95 mW cm^{-2} in the 400–1050 nm range. All the experiments were carried out at 30°C . Fig. 1 shows the irradiation spectrum of the solar simulator (1500W) and the used photoreactors.

For all the runs the alcohol initial concentration was 0.60 mM ; the pH was adjusted before each run at 1, 7 and 13 by employing HCl and NaOH solutions. The catalyst amount was 0.20 g L^{-1} ; this amount guaranteed that all the catalyst particles were irradiated. Before switching the lamp on, the suspension was stirred for 30 min at room temperature in order to reach the thermodynamic adsorption equilibrium. The contact of the suspension with the atmospheric air guaranteed that the aqueous solution was saturated by oxygen. During the run, samples of reacting suspension were withdrawn at fixed time intervals; they were immediately filtered through a $0.45 \mu\text{m}$ hydrophilic membrane (HA, Millipore) before being analysed.

The quantitative determination and identification of the species present in the reacting suspension were performed by means of a Shimadzu HPLC (Prominence LC-20A model and SPD-M20A Photodiode Array Detector), equipped with a Phenomenex Synergi 4 μm Hydro-RP 80A column at 313 K, using Sigma Aldrich standards. Retention times and UV-vis spectra of the compounds were compared with those of standards. The eluent consisted of: 50% methanol and 50% 13 mM trifluoroacetic acid aqueous solution. The flow rate was $0.40 \text{ cm}^3 \text{ min}^{-1}$. All the used chemicals were purchased from Sigma Aldrich with a purity of at least 98.0%.

3. Results and discussion

3.1. Catalyst characterization

XRD patterns of pristine and metal loaded Degussa TiO₂ photocatalysts showed the same crystalline phases, that were not influenced by the photodeposition of the metals, as expected (Fig. 2). The XRD patterns show that Degussa P25 is a well-crystallized mixture of anatase and rutile phases as indicated by the sharp diffraction peaks [4]. The peaks at $2\theta = 25.58^\circ$, 38.08° , 48.08° and 54.58° are characteristic of anatase phase and those at $2\theta = 27.51^\circ$, 36.51° , 41.1° , 54.11° and 56.51° of rutile [4]. The diffraction peaks of the metals are not detectable because of their limited amount ($\leq 1\%$).

The primary crystallite sizes of all the samples are 26.5 nm for anatase and 18.2 nm for rutile crystal (calculated by using the Scherrer equation). These figures are in agreement with TEM observations (Fig. 3), although a limited occurrence of bigger nanoparticles (up to diameters of ca. 70 nm) should also be noticed. The TEM images (Fig. 3) show that the metals loaded on TiO₂ catalysts are well distributed on the catalyst surface; the size of metal particles is in the 1–3 nm range. The size of the aggregates is in the 40–70 nm range, as determined by SEM observations (Fig. 4). Both TEM and SEM observations did not highlight noteworthy differences among the different samples.

UV-vis spectra of the metal loaded photocatalysts are reported in Fig. 5; Degussa P25 spectrum is also reported for comparison. The spectra show that all the samples have a good absorbance under UV irradiation, while just metal loaded samples have also good absorbance under visible irradiation.

3.2. Photoreactivity

No oxidation of alcohols was observed in the absence of irradiation or oxygen for runs carried out under the same experimental conditions employed for the photocatalytic ones. Irradiation, cata-

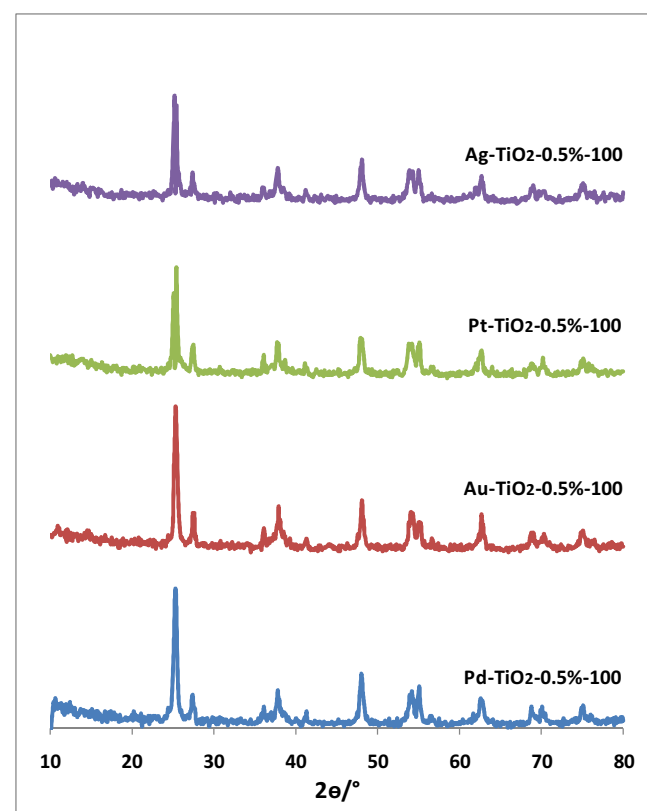


Fig. 2. XRD patterns of prepared metal loaded Degussa P25 photocatalysts.

lyst and oxygen were all needed for the oxidation of the substrates and the catalysts were stable in cycles of repeated runs, as expected for stable samples such as TiO₂ P25 and noble metals in their zero-oxidation state. In homogenous conditions, i.e. in the absence of catalyst, a negligible activity was observed.

Adsorption of the alcohols under dark conditions was always quite low, i.e. less than 3%. For all the used catalysts the main products of alcohol photocatalytic oxidation were the corresponding aldehydes (*p*-anisaldehyde, (PAA) or *p*-nitrobenzaldehyde), acids (*p*-methoxybenzoic acid or *p*-nitrobenzoic acid) and CO₂.

The experimental results obtained at different pH's for the MBA oxidation by metal loaded and un-loaded TiO₂ catalysts are reported in Table 1 as the half-life time of MBA, the selectivity to aldehyde calculated for 50% conversion. Selectivity values were calculated as the ratio between the produced moles of products (aldehyde or acid) and the reacted moles of substrate.

Unexpectedly, very selective (ca.100%)and fast PAA synthesis from MBA have been achieved at pH=1. The reaction rates of the reaction performed in neutral (pH=7) and basic conditions (pH=13) are smaller and close to each other, and the selectivities are lower than that at pH=1 (Table 1).

Activity and selectivity results of Ag- and Pt-loaded TiO₂ catalysts in neutral and basic conditions are close to un-loaded TiO₂, while at pH=1 metal loaded ones are more active than un-loaded Degussa P25. In acidic medium Au- and Pd-loaded TiO₂ showed activity and selectivity very similar to bare TiO₂, while under neutral and basic conditions they showed worse activity and selectivity than those of Degussa P25. These results indicate that Au and Pd loadings do not improve TiO₂ catalytic activity for PAA synthesis.

Pt-TiO₂-0.5%-100 showed the best performance, by assessing both selectivity and activity. In order to investigate the influence of the treatment temperature on the catalyst activity, this catalyst was also calcined at 400°C for 3 h. The Pt-TiO₂-0.5%-400 sample showed better results than Pt-TiO₂-0.5%-100, most probably due

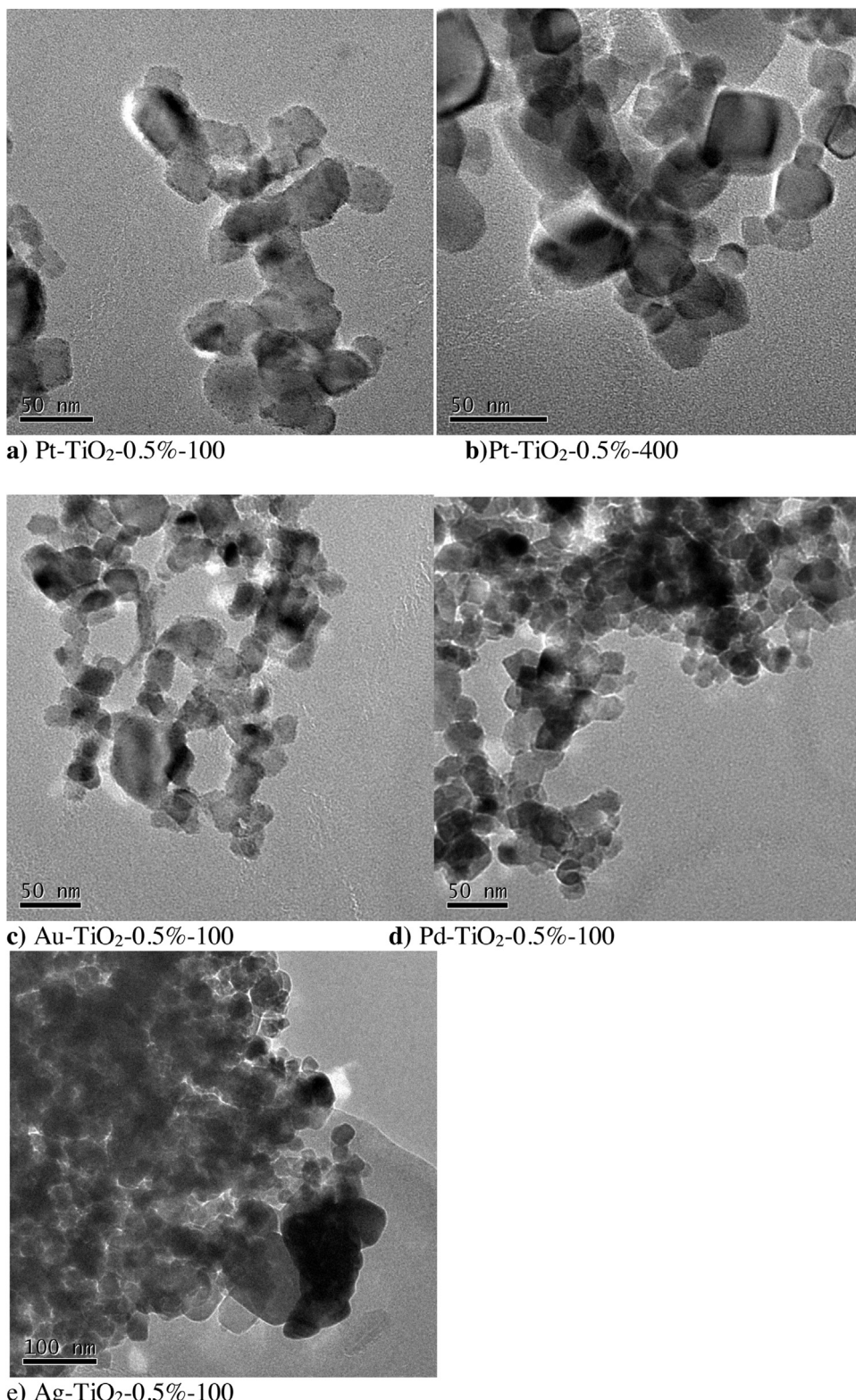


Fig. 3. TEM images of Pt-TiO₂-0.5%-100 (a), Pt-TiO₂-0.5%-400 (b) Au-TiO₂-0.5%-100 (c), Pd-TiO₂-0.5%-100 (d), Ag-TiO₂-0.5%-100 (e).

to an improved contact between the loaded metal particles and TiO₂. By using this catalyst, 71% selectivity for PAA production was obtained even at neutral pH with a higher activity ($t_{1/2} = 1.6$ vs. 2.1 h). For all the used catalysts and in any experimental conditions, the obtained 4-methoxybenzoic acid selectivity was always very low (<1%).

The Pt-TiO₂-0.5%-400 catalyst has also been used for the NBA oxidation runs, which were carried out in order to investigate the influence of the substituent group of the aromatic ring on the photoactivity. Fig. 6 shows experimental results of photocatalytic oxidation of NBA to NBAD and 4-nitrobenzoic acid by using Pt-TiO₂-0.5%-400 photocatalyst at pH=13. This Figure reports the NBA, NBAD and 4-nitrobenzoic acid concentrations versus the irradi-

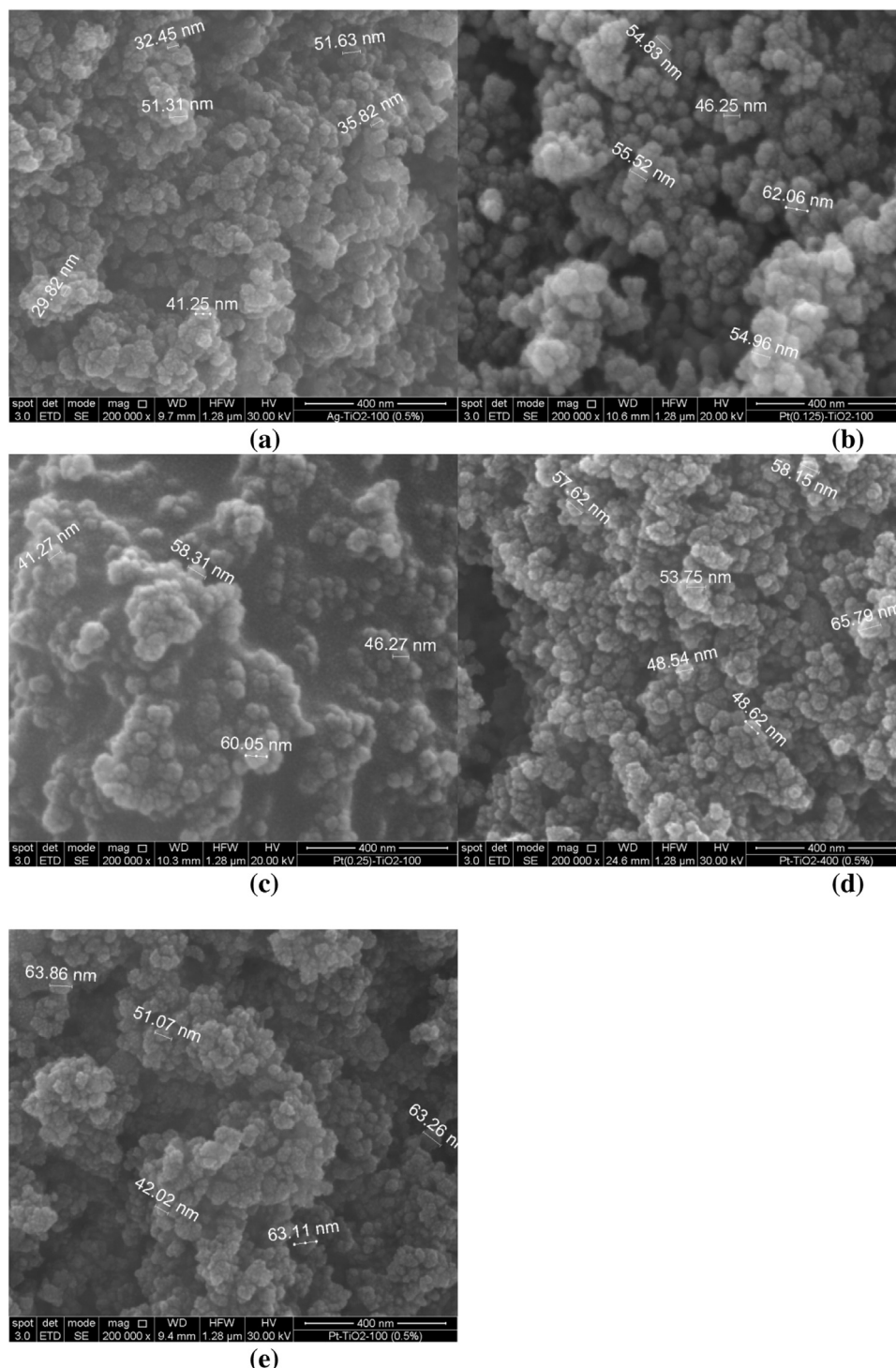


Fig. 4. SEM image (magnification: x200000) of Ag-TiO₂-%0.5-100 (a), Pt-TiO₂-%0.125-100 (b), Pt-TiO₂-%0.25-100 (c), Pt-TiO₂-%0.5-100 (d), Pt-TiO₂-%0.5-400 (e) photocatalysts.

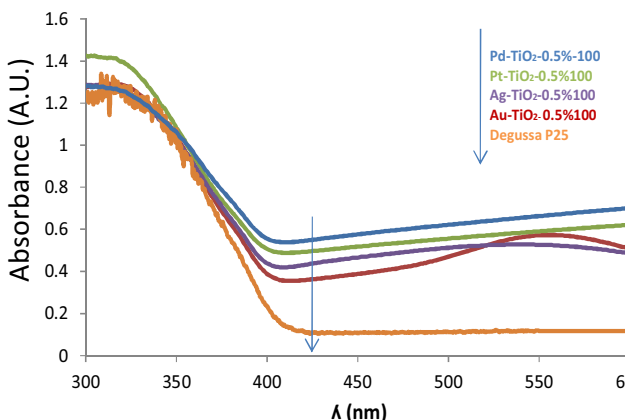
ation time; the calculated values of NBA conversion and selectivity to NBAD and 4-nitrobenzoic acid are illustrated as well. It may be noted that, by increasing the alcohol conversion, the aldehyde production also increases up to a 30% conversion, afterwards it starts decreasing due to overoxidation of NBAD to 4-nitrobenzoic acid. For this reason, aldehyde selectivity continuously decreases, while acid selectivity increases. The experimental results obtained at different pH's for the NBA oxidation by Pt-TiO₂-0.5%-400 and Degussa P25 catalysts are reported in Table 2, along with the half-life time of

NBA, the selectivity to aldehyde and to acid calculated for 50% conversion. To the sake of comparison, Table 2 also reports the results obtained with MBA. From these data one can conclude that Pt-TiO₂-0.5%-400 produced better results than bare TiO₂, for both MBA and NBA oxidations. In particular, higher selectivities were recorded in the formation of the corresponding aldehydes for both alcohols, especially in acidic media. For instance, at pH = 1, PAA selectivity was 99%, while 4-nitrobenzaldehyde (NBAD) selectivities were 75% and 85% for bare TiO₂ and Pt-TiO₂-0.5%-400, respectively. How-

Table 1

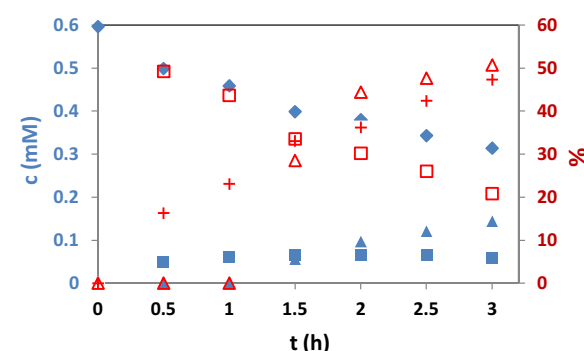
Photoreactivity results obtained under solar irradiation. MBA initial concentration: 0.6 mM; catalyst amount: 0.20 g L⁻¹. t_{1/2} and selectivity values were calculated for 50% conversion.

Catalyst	pH	t _{1/2} (h)	Aldehyde Selectivity (%)
Homogenous	1	negligible conv.	
Degussa P25	1	0.83	100
Degussa P25	7	2.0	15
Degussa P25	13	1.7	27
Au-TiO ₂ -0.5%-100	1	0.80	100
Au-TiO ₂ -0.5%-100	7	3.0	17
Au-TiO ₂ -0.5%-100	13	2.3	32
Pd-TiO ₂ -0.5%-100	1	0.70	100
Pd-TiO ₂ -0.5%-100	7	3.9	30
Pd-TiO ₂ -0.5%-100	13	2.6	29
Ag-TiO ₂ -0.5%-100	1	0.53	100
Ag-TiO ₂ -0.5%-100	7	3.5	15
Ag-TiO ₂ -0.5%-100	13	1.8	12
Ag-TiO ₂ -1%-100	1	0.75	100
Ag-TiO ₂ -1%-100	7	2.5	13
Ag-TiO ₂ -1%-100	13	2.1	21.5
Pt-TiO ₂ -0.5%-100	1	0.5	100
Pt-TiO ₂ -0.5%-100	7	2.1	30
Pt-TiO ₂ -0.5%-100	13	2.5	33
Pt-TiO ₂ -0.25%-100	1	0.45	100
Pt-TiO ₂ -0.125%-100	1	0.45	85
Pt-TiO ₂ -0.5%-400	1	0.45	100
Pt-TiO ₂ -0.5%-400	7	1.6	71
Pt-TiO ₂ -0.5%-400	13	2.1	30
Pt-TiO ₂ -1%-400	1	1	95

**Fig. 5.** UV-vis diffuse reflectance spectra of Pd, Pt, Ag, and Au loaded TiO₂ photocatalysts.**Table 2**

Photoreactivity results obtained under solar irradiation. Aromatic alcohol initial concentration: 0.60 mM; catalyst amount: 0.20 g L⁻¹. t_{1/2} and selectivity values were calculated for 50% conversion.

Catalyst	Substrate	pH	t _{1/2} (h)	Aldehyde Selectivity (%)	Acid Selectivity (%)	Total product selectivity (%)
Degussa P25	MBA	1	0.83	100	–	100
Degussa P25	MBA	7	2.0	50	0.6	15
Degussa P25	MBA	13	1.7	27	0.7	28
Degussa P25 ^a	NBA	1	%19 Conv.	75	13	88
Degussa P25	NBA	7	5.0	18	1.2	19
Degussa P25	NBA	13	2.1	30	53	83
Pt-TiO ₂ -0.5%-400	MBA	1	0.45	100	–	100
Pt-TiO ₂ -0.5%-400	MBA	7	1.6	71	0.8	72
Pt-TiO ₂ -0.5%-400	MBA	13	2.1	30	0.5	31
Pt-TiO ₂ -0.5%-400 ^a	NBA	1	%14 Conv.	85	14	99
Pt-TiO ₂ -0.5%-400	NBA	7	5.3	55	14	69
Pt-TiO ₂ -0.5%-400	NBA	13	3.4	21	52	73

^a These values were calculated for 3 h of irradiation due to their low conversion.**Fig. 6.** Experimental results of photocatalytic oxidation of NBA (◊) to NBAD (■) and 4-nitrobenzoic acid (▲) by using Pt-TiO₂-0.5%-400 (0.2 g/L) photocatalyst at pH = 13. Conversion (+), selectivity to NBAD (□) and selectivity to 4-nitrobenzoic acid (△) values are quoted on the right ordinate axis.

ever, at pH = 1, the reaction rate of NBA oxidation was very low. After 3 h irradiation, just 19% and 14% conversions were obtained by using the bare and loaded catalyst, respectively.

The reactivity for NBA oxidation grows by increasing pH. In addition, along with NBAD a significant amount of 4-nitrobenzoic acid was also obtained. NBAD selectivity was very high (52–53%) by using both catalysts at pH = 13. From the results reported in Table 2, it may be noted that at pH = 1 the total selectivity (for both aldehyde and acid production) is 100% for Pt-TiO₂-0.5%-400 and 88% for Degussa P25. Similarly, at pH = 13 a high total selectivity was obtained. However, at neutral conditions, Degussa P25 showed markedly a low total selectivity (19%), while Pt-TiO₂-0.5%-400 showed a total selectivity value of 69%. These results show that Pt loading improves not only the reaction rate, but also the product selectivity in these green conditions, which importantly do not require modifying the pH to values far from the neutrality.

The different reactivity results obtained with MBA and NBA can be analyzed by considering the different nature of the substituent groups in MBA and NBA. MBA includes an electron donor group (methoxy), whereas NBA carries a nitro-group, which is electron withdrawing, and this difference could be a reason of the different performance highlighted in Table 2. In the presence of an electron donor group, as methoxy, the reaction rate is fast in acidic medium, whereas in the presence of electron withdrawing group, as nitro, the reaction rate is fast in basic medium. Moreover, in the presence of a nitro group, unlike the case of methoxy, a significant amount of 4-nitrobenzoic acid was obtained. The amount of this acid is very high especially in highly basic conditions, owing to the fact that OH radicals, prevalently formed in a basic medium, crucially promote

its formation. On the contrary, NBAD formation is more preferred in acidic medium. Unlike NBA oxidation, a negligible amount of 4-methoxybenzoic acid was obtained from MBA oxidation. This result can be explained by considering that the main oxidation product of MBA, i.e. PAA, mainly degrades to open ring products and CO₂, rather than undergoing oxidation to 4-methoxybenzoic acid, as demonstrated by *ad hoc* tests performed starting with PAA as the reactant. Finally, we can notice that nitro-group is also responsible for the decrease of the reactivity, in agreement with recent published evidence [21,22]. Previous research works reported that the mineralization of adsorbed aromatic alcohol molecules proceeds through steps in which the oxidation products are not released into the liquid phase, suggesting that this process should be favoured by using a catalyst with a hydrophobic surface [20,23]. However, in the present work, the experimental results show that by adjusting pH, green synthesis is achievable selectively even on TiO₂ catalysts owning a given hydrophobic character.

4. Conclusions

Pt, Au, Ag and Pd loaded Degussa P25 TiO₂ samples were prepared by the photoreduction method, characterised and used for partial photocatalytic oxidation of MBA and NBA at different pH's. pH effects on alcohol activity and product selectivity mainly depend on the electron donor or electron withdrawing character of the substituent groups. Pt loaded catalyst (Pt-TiO₂-0.5%- 400) could be useful for very selective and active benzyl alcohols oxidations under totally green conditions: under sunlight, in water and even in neutral conditions. Green synthesis is achievable selectively even on TiO₂ catalysts with hydrophobic surfaces by adjusting pH.

Acknowledgments

The article is dedicated to the career of prof. Vincenzo Augugliaro (University of Palermo, Italy) in the occasion of his retirement.

Authors thank the TÜBİTAK (Project no: 111T489) for financial support.

Authors thank for TEM experimental data were provided by Centro Grandi Apparecchiature—UniNetLab—Università di Palermo.

References

- [1] Heterogeneous Photocatalysis, in: M. Schiavello (Ed.), first ed., Wiley, Chichester, 1997.
- [2] V. Augugliaro, G. Camera-Roda, V. Loddo, G. Palmisano, L. Palmisano, J. Soria, S. Yurdakal, *J. Phys. Chem. Lett.* 6 (2015) 1968–1981.
- [3] S. Yurdakal, V. Augugliaro, V. Loddo, G. Palmisano, L. Palmisano, *New J. Chem.* 36 (2012) 1762–1768.
- [4] B.S. Tek, S. Yurdakal, L. Özcan, V. Augugliaro, V. Loddo, G. Palmisano, *Sci. Adv. Mater.* 7 (2015) 2306–2319.
- [5] J.M. Thomas, W.J. Thomas, *Principle and Practice of Heterogeneous Catalysis*, second ed., VCH, Germany, 1997.
- [6] G. ten Brink, I.W.C.E. Arends, R.A. Sheldon, *Science* 287 (2000) 1636–1639.
- [7] C. Li, L. Chen, *Chem. Soc. Rev.* 35 (2006) 68–82.
- [8] Z. Zheng, B. Huang, X. Qin, X. Zhang, Y. Dai, M.H. Whangbo, *J. Mater. Chem.* 21 (2011) 9079–9087.
- [9] J. Scott, W. Irawaty, G. Low, R. Amal, *Appl. Catal. B: Environ.* 164 (2015) 10–17.
- [10] A. Bumajdad, M. Madkour, *Phys. Chem. Chem. Phys.* 16 (2014) 7146–7158.
- [11] P. Wang, B. Huang, Y. Dai, M.H. Whangbo, *Phys. Chem. Chem. Phys.* 14 (2012) 9813–9825.
- [12] S. Sarina, E.R. Waclawik, H. Zhu, *Green Chem.* 15 (2013) 1814–1833.
- [13] T. Morikawa, T. Ohwaki, K.-i. Suzuki, S. Moribe, S. Tero-Kubota, *Appl. Catal. B: Environ.* 83 (2008) 56–62.
- [14] E. Grabowska, J. Reszczyńska, A. Zaleska, *Water Res.* 46 (2012) 5453–5471.
- [15] F. Ruggieri, D. Di Camillo, L. Maccarone, S. Santucci, L. Lozzi, *J. Nanopart. Res.* 15 (2013) 1982.
- [16] W. Kim, T. Tachikawa, H. Kim, N. Lakshminarasimhan, P. Murugan, H. Park, T. Majima, W. Choi, *Appl. Catal. B Environ.* 147 (2014) 642–650.
- [17] X. Lang, X. Chen, J. Zhao, *Chem. Soc. Rev.* 43 (2014) 473–486.
- [18] Y. Shiraishi, H. Sakamoto, Y. Sugano, S. Ichikawa, T. Hirai, *ACS Nano* 7 (2013) 9287–9297.
- [19] Y. Shiraishi, H. Sakamoto, K. Fujiwara, S. Ichikawa, T. Hirai, *ACS Catal.* 4 (2014) 2418–2425.
- [20] L. Palmisano, V. Augugliaro, M. Bellardita, A. Di Paola, E. García López, V. Loddo, G. Marci, G. Palmisano, S. Yurdakal, *ChemSusChem* 4 (2011) 1431–1438.
- [21] S. Yurdakal, G. Palmisano, V. Loddo, O. Alagöz, V. Augugliaro, L. Palmisano, *Green Chem.* 11 (2009) 510–516.
- [22] S. Yurdakal, V. Augugliaro, *RSC Adv.* 2 (2012) 8375–8380.
- [23] S. Yurdakal, G. Palmisano, V. Loddo, V. Augugliaro, L. Palmisano, *J. Am. Chem. Soc.* 130 (2008) 1568–1569.
- [24] R.J. Bickley, T. Gonzalez-Carreno, J.S. Lees, L. Palmisano, R.J.D. Tilley, *J. Solid State Chem.* 92 (1991) 178–190.
- [25] D. Vione, C. Minerio, V. Maurino, M.E. Carlotti, T. Picatontto, E. Pelizzetti, *App. Catal. B: Environ.* 58 (2005) 79–88.
- [26] T.A. Egerton, J.A. Mattinson, *J. Photochem. Photobiol. A: Chem.* 194 (2008) 283–289.
- [27] Y. Wang, J. Yu, W. Xiao, Q. Li, *J. Mater. Chem. A* 2 (2014) 3847–3855.
- [28] L. Di, Z. Xu, X. Zhang, *Catal. Today* 211 (2013) 143–146.